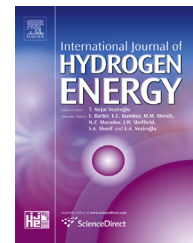


Available online at [www.sciencedirect.com](http://www.sciencedirect.com)

ScienceDirect

journal homepage: [www.elsevier.com/locate/he](http://www.elsevier.com/locate/he)

# Performance investigation of hydrogen production by the flat-plate collectors assisted by a solar pond

Mustafa Erden <sup>a,1</sup>, Mehmet Karakilcik <sup>a,\*</sup>, Ibrahim Dincer <sup>b</sup>

<sup>a</sup> Department of Physics, Faculty of Sciences and Letters, University of Cukurova, Adana 01330, Turkey

<sup>b</sup> Faculty of Engineering and Applied Science, University of Ontario Institute of Technology (UOIT), 2000 Simcoe Street, North Oshawa, Ontario, L1H 7K4, Canada

## ARTICLE INFO

### Article history:

Received 8 February 2016

Received in revised form

7 April 2016

Accepted 18 April 2016

Available online xxx

### Keywords:

Hydrogen production

Solar energy

Multi-generation

Energy and exergy efficiency

## ABSTRACT

In this study, an integrated model system which is consisted of a solar pond, flat-plate collectors and an organic Rankine cycle (ORC) was designed to determine not only thermal and electricity but also hydrogen generation performances. The flat-plate collectors assisted by a solar pond to enhanced the thermal performance of the system in order to generate electrical energy with ORC. In addition, mass, enthalpy, entropy, energy and exergy balance equations of the system was solved by using a software which is called Engineering Equation Solver (EES). Thus, the thermodynamic analysis of the system were done. As a result, a significant amount of electrical energy is produced by using ORC which works with the thermal energy comes from the integrated system. Thus, this system can reach up to a hydrogen production rate of 2.25 kg/day by the water electrolysis system. The results show that hydrogen production performance increased by increasing the performance of the thermal system. Thus, the performance of a solar pond is an important effects at the performance of the integrated system. We believe that the theoretical results obtained in this work are very useful for making realistic and accurate predictions about the pre-planned integrated systems to produce the hydrogen energy.

© 2016 Hydrogen Energy Publications LLC. Published by Elsevier Ltd. All rights reserved.

## Introduction

Solar ponds that can supply and store thermal energy for many applications. A solar pond contains salty water whose salinity increases with depth, forming a saline concentration gradient. The added salt into the bottom layer of the pond inhibits natural convection, allowing the cooler and fresh water on top to act as insulation and reduce evaporation. Thus, solar energy reaching the bottom of the pond is trapped

and stored there. The performance of a solar pond depends on the heat storage capacity of the salty water, thermo-physical properties of the pond and surrounding conditions [1].

Karakilcik et al. [2] investigated the performance of a solar pond by experimentally and theoretically. They found that the temperature of each layer of the inner zones depends on the incident radiation, zone thicknesses, shading areas of the zones and overall heat loss. The modification of the zone thicknesses increases pond performance and stability of the pond.

\* Corresponding author. Tel.: +90 322 3386084; fax: +90 322 3386070.

E-mail addresses: [kkilcik@cu.edu.tr](mailto:kkilcik@cu.edu.tr) (M. Karakilcik), [ibrahim.dincer@uoit.ca](mailto:ibrahim.dincer@uoit.ca) (I. Dincer).

<sup>1</sup> Tel.: +90 322 3386084; fax: +90 322 3386070.

<http://dx.doi.org/10.1016/j.ijhydene.2016.04.116>

0360-3199/© 2016 Hydrogen Energy Publications LLC. Published by Elsevier Ltd. All rights reserved.

Bozkurt et al. [3] investigated heat storage performance of integrated solar pond and collectors. A cylindrical solar pond system with a radius of 0.80 m and a depth of 2 m and four flat-plate collectors whose dimensions of 1.90 m × 0.90 m was used. Their results showed that pond's heat storage performance is affected strongly by the number of collectors. As a result, they obtained a good agreement between experimental and theoretical efficiency profiles.

Date et al. [4] compared of the transient thermal performance of solar pond with heat extraction from lower convective zone (LCZ) alone and that with combined heat extraction from LCZ and non-convective zone (NCZ). Their study showed that the instantaneous efficiency curves tend to flatten out with increased heat extraction for both LCZ alone and combined NCZ and LCZ heat extraction. They also found that the temperature of LCZ and the average annual solar pond efficiency is very sensitive to the mass flux of the heat transfer fluid that flows through the in-pond heat exchanger.

Flat-plate collectors that are devices employed to gain useful heat energy from the incident solar radiation. A typical flat-plate collector consists of an absorber metal sheet of high thermal conductivity, with integrated or attached riser tubes in an insulated box together with transparent glazing. The absorber metal sheet absorbs solar radiation and converts it into heat energy. This heat energy is then absorbed by the working fluid that passes through the riser tubes [5].

Farahat et al. [6] developed an exergetic optimization of flat-plate solar collectors to determine the optimal performance and design parameters of these solar to thermal energy conversion systems. They carried out a detailed energy and exergy analysis for evaluating the thermal and optical performance, exergy flows and losses as well as exergetic efficiency for a typical flat-plate solar collector under given operating conditions. They found the optimum values of the mass flow rate, the absorber plate area and the maximum exergy efficiency.

Dikici et al. [7] investigated the solar-assisted heat pump system with flat-plate collectors experimentally and they tested it for domestic space heating. They found the system COP as 3.08 while the exergy loss of the solar collectors as 1.92 kW. They also reported that the energy and exergy loss analysis results show that the COP increase when the exergy loss of evaporator decrease.

Ahmadi et al. [8] reported a comprehensive thermodynamic analysis and multi-objective optimization of an ocean thermal energy conversion (OTEC) system which drives a low-temperature organic Rankine cycle to produce hydrogen using electrolysis. They used a fast and elitist non-dominated sorting genetic algorithm (NSGA-II) to determine the best design parameters for the system. They showed that the system performance is notably affected by the mass flow rate of warm ocean surface water, solar radiation intensity, condenser temperature and evaporator pinch point temperature difference.

Bicer et al. [9] proposed a new combined system, using solar and geothermal resources, for hydrogen production. This combined renewable energy system consists of solar PV/T modules and an organic Rankine cycle. They found the overall energy and exergy efficiencies of the system can reach up to 10.8% and 46.3% respectively for a geothermal water temperature of 210 °C.

Bozoglan et al. [10] studied some technical issues related to solar hydrogen production methods such as exergy-based environmental and sustainability parameters and found exergetic benign index to be 6.30. Accordingly, they stated that solar hydrogen production should be used for practical applications because of higher exergetic sustainability potential and lower environmental destruction index.

Joshi et al. [11] considered a solar-based thermally-driven hydrogen production system and analyzed thermodynamically. They also investigated the effects of environmental conditions and relevant parameters on the energy and exergy efficiencies of the system. They reported that the overall energy and exergy efficiencies of the solar thermal hydrogen production system can be evaluated as 14.25% and 6.12%, respectively.

Flat-plate collectors have been used to provide hot water for domestic and industrial usage. Especially for industrial use large amounts of hot water may be required in a short time. At this point, the performance of the flat-plate collectors may be insufficient. This trouble can be resolved by using a process as preheating of inlet water by using a solar pond. Here the performance of the solar pond will be one of the important parameters affecting the performance of the system. To date there have not been any theoretical analysis on the integrated system of flat-plate collectors assisted by a solar pond. This is the main purpose behind the present study.

The objective of the study is to point out the performance of hydrogen production of a new integrated system. The system was design to produce electric and hydrogen from the electrolysis and ORC integrated with the flat-plate collectors assisted by a solar pond. Thermodynamic analysis of the integrated system was studied theoretically. The pre-heat energy which was obtained from solar pond in order to enhanced the heat performance of the collectors. Increasing the heat performance of thermal system was increased amount of the electric produced by ORC and also amount of the hydrogen produced by the electrolysis. Therefore, flat-plate collectors assisted by a solar pond is significantly effected electric and hydrogen performance on the integrated system in a day. A detail study is conducted on the energy and exergy efficiencies of the system components.

## System description and analysis

The present system, as shown schematically in Fig. 1, comprises a salinity gradient solar pond, in-pond heat exchangers, flat-plate solar collectors, an ORC which contains ammonia as a working fluid to generate electricity and electrolysis system to produce hydrogen. The solar pond equipped with flat plate collectors are used as solar thermal energy collectors. Exchanger-1 is used for heat extraction from the lower convective zone (LCZ) while exchanger-2 is used for heat rejection to the upper convective zone (UCZ) of the pond. The solar pond and flat-plate solar collectors incorporate an ORC which evaporates a working fluid to drive a turbine to generate electricity, which in turn is used to drive electrolysis system to produce hydrogen. After passing through the turbine, the vapor is then condensed back to a liquid through the condenser and pumped back through the evaporator, and the

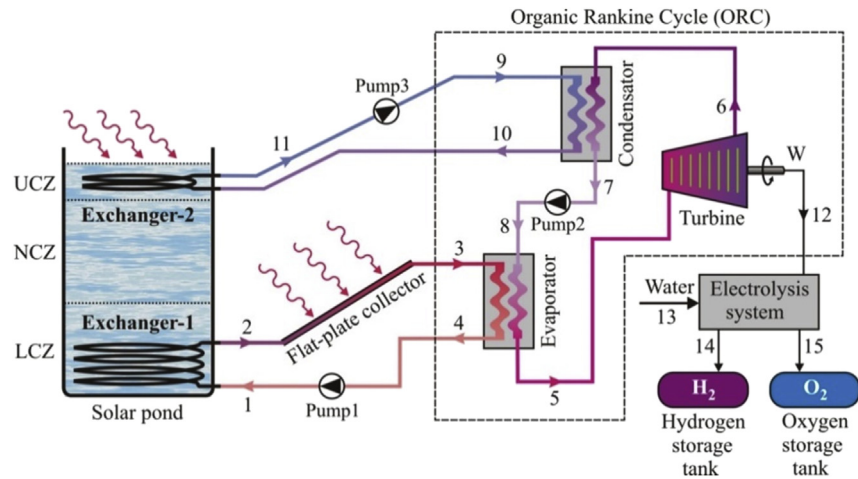


Fig. 1 – Schematic of the integrated system.

cycle is repeated continuously. Energy and exergy analyses are used to determine the efficiency of the integrated system. Therefore, the relevant equations for the integrated system are described in the following subsections.

#### Solar pond

Solar energy in the form of heat is collected and stored in the solar pond which can be confidently used as a source of heat for industrial processes and the generation of electricity. A solar pond consists of three layers of water, as shown in Fig. 2, which are upper convective zone (UCZ), non-convective zone (NCZ) and lower convective zone (LCZ) or in other words heat storage zone (HSZ). The UCZ is a homogenous thin layer of low salinity brine or fresh water at the top of the pond. The UCZ is fed with fresh water to maintain cleanliness of the pond and replenish lost water due to evaporation. The NCZ is a thermal insulator at the middle of the pond which has salinity gradient with salinity increases from top to bottom of this layer. The NCZ plays an important role to the working of a solar pond by allowing an extensive amount of solar radiation to the bottom of the pond and prevents the heat loss by natural convection. The LCZ is a heat storage region which contains salty water

with the highest density at the bottom of the pond. The LCZ absorbs and stores an important amount of solar energy in the form of heat. Therefore this zone has the highest temperature and heat has been extracted from the LCZ [3,12].

According to the energy flows throughout the layers of the solar pond as shown in Fig. 3, the general energy balance for the LCZ can be written as:

$$\dot{Q}_{LCZ,stored} = \dot{Q}_{LCZ,in} - \dot{Q}_{LCZ,bottom} - \dot{Q}_{LCZ,up} - \dot{Q}_{LCZ,side} - \dot{Q}_{LCZ,ext} \quad (1)$$

where  $\dot{Q}_{LCZ,stored}$  is the heat stored in the LCZ,  $\dot{Q}_{LCZ,in}$  is the amount of the solar radiation entering the LCZ,  $\dot{Q}_{LCZ,bottom}$  is the heat loss to the bottom wall from the LCZ,  $\dot{Q}_{LCZ,up}$  is the heat loss to the NCZ from the LCZ and  $\dot{Q}_{LCZ,side}$  is the heat loss to the side wall from the LCZ and  $\dot{Q}_{LCZ,ext}$  is the heat loss by extraction.

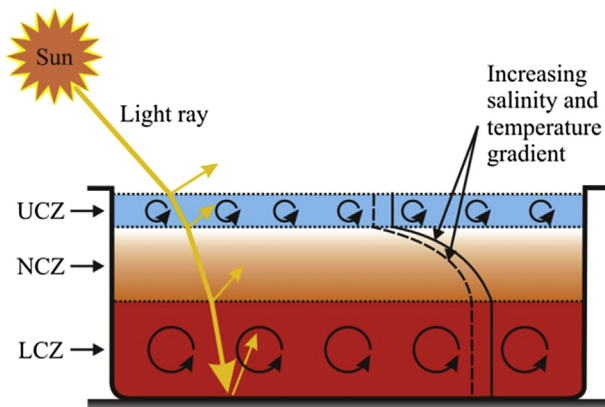


Fig. 2 – Schematic vertical cross-section through a salt gradient solar pond.

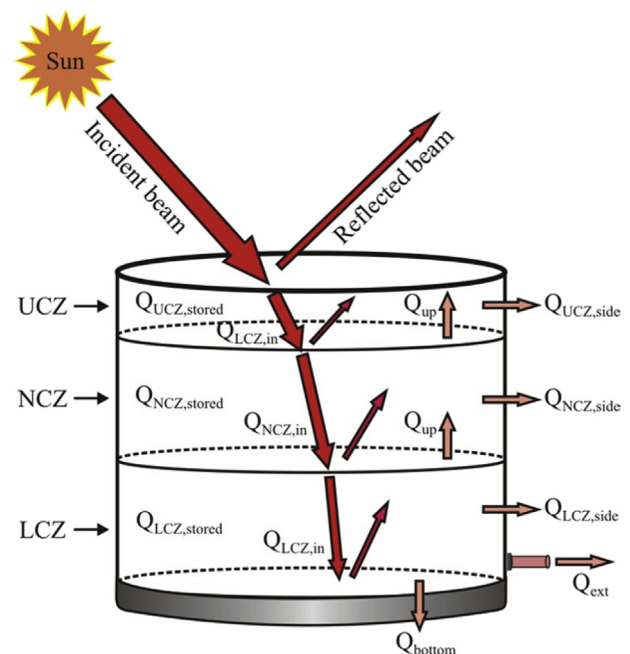


Fig. 3 – Schematic of the energy flows for the solar pond.

$$\dot{Q}_{LCZ,in} = \beta i A_{LCZ} ((1 - F)h(X - \delta)) \quad (2)$$

where  $\beta$  is the fraction of the incident solar radiation that enters the solar pond,  $i$  is the total solar radiation reaching the solar pond surface ( $W/m^2$ ),  $A_{LCZ}$  is the sunny area of the LCZ ( $m^2$ ),  $F$  is the absorbed energy fraction at a region of  $\delta$  thickness ( $m$ ),  $h$  is the solar radiation flux absorbed ( $W/m^2$ ). The transmission coefficient for air-water interface depends on the angle of incidence and refractive of sunlight, varying slightly with radiation wavelength, time of the day, water temperature and salinity [13]. So, the fraction of the solar radiation is given as:

$$\beta = 1 - 0.5 \left[ \frac{\sin^2(\theta_i - \theta_r)}{\sin^2(\theta_i + \theta_r)} + \frac{\tan^2(\theta_i - \theta_r)}{\tan^2(\theta_i + \theta_r)} \right] \quad (3)$$

where  $\theta_i$  is the incidence angle and  $\theta_r$  is the refraction angle.

$$h(X - \delta) = 0.727 - 0.056 \left( \frac{X_3 - \delta}{\cos \theta_r} \right) \quad (4)$$

The energy efficiency of a solar pond has been defined as the ratio of the total thermal energy extracted to the total incident solar radiation within a specified time interval. Thus, energy efficiency of the solar pond is given as:

$$\eta_{en} = \frac{\dot{Q}_{LCZ,stored}}{\dot{Q}_{LCZ,in}} = 1 - \frac{(\dot{Q}_{LCZ,bottom} + \dot{Q}_{LCZ,up} + \dot{Q}_{LCZ,side})}{\dot{Q}_{LCZ,in}} \quad (5)$$

where

$$\dot{Q}_{LCZ,bottom} = \frac{k_{side} A}{\Delta X_{LCZ,bottom}} (T_{LCZ} - T_a) \quad (6)$$

$$\dot{Q}_{LCZ,up} = \frac{k_w A}{\Delta X_{LCZ,up}} (T_{LCZ} - T_{NCZ}) \quad (7)$$

$$\dot{Q}_{LCZ,side} = \frac{k_{side} (2\pi L_{LCZ})}{\ln \left[ \frac{r_{out}}{r_{in}} \right]} (T_{LCZ} - T_a) \quad (8)$$

where  $\Delta X$  is the thickness of the sub divisions of the LCZ ( $r_{in}$  and  $r_{out}$  is the inner and outer radius of the solar pond, respectively).

More information about solar pond is detailed in Refs. [2–5].

### Heat exchanger

Heat exchangers are devices that facilitate the exchange of heat between two fluids at different temperatures that are separated by a solid wall. The rate of heat transfer in a heat exchanger can be expressed in an analogous manner to Newton's law of cooling as [14]:

$$\dot{Q}_{exc} = U A_s \Delta T_m \quad (9)$$

where,  $U$  is the overall heat transfer coefficient ( $W/m^2 \cdot ^\circ C$ ) that accounts for the contribution of the effects on heat transfer such as convection and conduction,  $A_s$  is the heat transfer area ( $m^2$ ),  $\Delta T_m$  is an appropriate average temperature difference between the two fluids ( $^\circ C$ ). However,  $U$  and  $\Delta T_m$  are vary along the heat exchanger. Therefore, log mean temperature

difference, which is the suitable form of the average temperature difference for use in the analysis of heat exchanger, is given as:

$$\Delta T_m = \frac{\Delta T_1 - \Delta T_2}{\ln \left( \frac{\Delta T_1}{\Delta T_2} \right)} \quad (10)$$

where

$$\Delta T_1 = T_{LCZ} - T_{exc-1,out} \quad (11)$$

$$\Delta T_2 = T_{LCZ} - T_{exc-1,in} \quad (12)$$

Here  $T_{LCZ}$  stands for the temperature of the LCZ of the pond,  $T_{exc-1,out}$  stands for the temperature of the outlet water from the exchanger-1 and  $T_{exc-1,in}$  stands for the temperature of the inlet water to the exchanger-1 as shown in Fig. 4. Likewise, for the exchanger-2 as shown in Fig. 1,  $\Delta T_1$  and  $\Delta T_2$  can be expressed as:

$$\Delta T_1 = T_{UCZ} - T_{exc-2,out} \quad (13)$$

$$\Delta T_2 = T_{UCZ} - T_{exc-2,in} \quad (14)$$

Here  $T_{UCZ}$  stands for the temperature of the UCZ of the pond,  $T_{exc-2,out}$  stands for the temperature of the outlet water from the exchanger-2 and  $T_{exc-2,in}$  stands for the temperature of the inlet water to the exchanger-2.

The heat gain of the flowing water in the heat exchanger in the rate form can be expressed as:

$$\dot{Q}_{exc} = \dot{m}_c (T_{exc,out} - T_{exc,in}) \quad (15)$$

The flowing water in the exchanger will gain practically the entire rate of heat transfer in the heat exchanger. Therefore, it can be expressed as:

$$U A_s (\Delta T_m) = \dot{m}_c (T_{exc,out} - T_{exc,in}) \quad (16)$$

Although the specific heat of a fluid ( $c_p$ ), in general, changes with temperature, it can be treated as a constant at some average value with little loss in accuracy. Therefore the temperature of water which flows through the heat exchanger was treated as average value of  $T_{exc,in}$  and  $T_{exc,out}$  to determine the value of  $c_p$ .

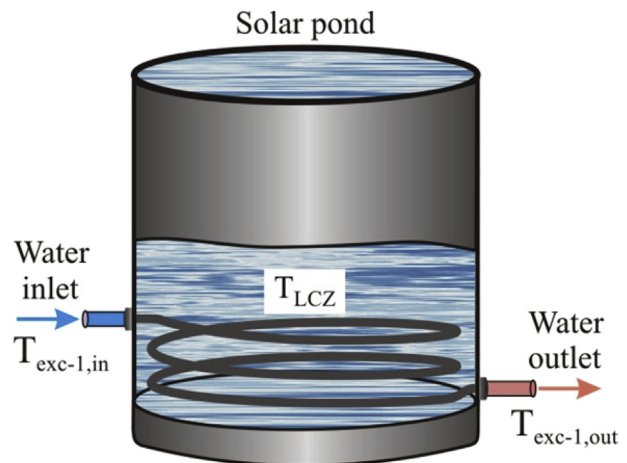


**Fig. 4 – Temperature representation of the water inlet, outlet and the LCZ of the pond.**

### Flat-plate collector

Flat-plate collectors are the most common solar collector that is used for residential water heating, and solar space heating. A typical flat-plate collector consists of heat absorbing riser tubes attached on an absorber plate in a collector housing covered with glazing sheet. The glazing sheet transmits significant amount of sunlight to the absorber plate although it reflects small amount of sunlight. In addition, the glazing sheet insulates the inner space of the collector housing from the current of air and protects it from dirty. The absorber plate which covers all the aperture area of the collector is made of a metal sheet of high thermal conductivity, such as copper, aluminum or steel, with heat absorbing riser tubes either integral or attached. Solar irradiance passing through the glazing sheet is absorbed directly onto the absorber plate whose surface is coated with a special selective material to absorb the maximum possible amount of solar irradiance while losing a minimum amount of heat back to the surroundings. The absorbing rising tubes transfer the heat from the absorber plate into the working fluid. The collector housing which is highly insulated at the back and sides to reduce heat losses from the back and sides of the collector is made of galvanized metal, wood or plastic [15].

As shown in Fig. 1, water enters the flat-plate solar collector at point 2. Therefore, the useful heat gained by the working fluid (water) can be expressed as:

$$\dot{Q}_u = \dot{m}C_p(T_3 - T_2) \quad (17)$$

where  $\dot{m}$ ,  $C_p$ ,  $T_3$  and  $T_2$  are the mass flow rate, specific heat at constant pressure, water outlet temperature and water inlet temperature, respectively.

The energy efficiency of the flat-plate solar collector is given by Ref. [16]:

$$\eta = \frac{\dot{Q}_u}{A_c \dot{I}} \quad (18)$$

where  $A_c$  is the aperture area of the collector, in  $m^2$ .

### Organic rankine cycle (ORC)

The ORC is an engine that uses an organic working fluid to generate electricity. The schematic of this engine is shown in Fig. 1. Such engine comprises four components: a pump, an evaporator or boiler, an expansion device or turbine to drive electricity generator and a condenser for heat rejection. Heat

is converted into work when the working fluid undergoes the following four processes. Process 7–8; pumping of the working fluid, process 8–5; heating the working fluid to the turbine inlet condition (vaporization), process 5–6; expansion of vaporized working fluid through the turbine to generate mechanical power, process 6–7; converting the working fluid leaving the turbine into a saturated liquid [17,18].

The net power output of the ORC system can be expressed as:

$$\dot{W}_{net} = \dot{W}_G - (\dot{W}_{pump1} + \dot{W}_{pump2} + \dot{W}_{pump3}) \quad (19)$$

where  $\dot{W}_G$  is the turbine generator power,  $\dot{W}_{pump1}$ ,  $\dot{W}_{pump2}$ ,  $\dot{W}_{pump3}$  are pumping powers.

The turbine generator power can be expressed as:

$$\dot{W}_G = \eta_T \eta_G \dot{m}_5 (h_5 - h_6) \quad (20)$$

where  $\eta_T$ ,  $\eta_G$ ,  $\dot{m}_5$ ,  $h_5$  and  $h_6$  are the turbine isentropic efficiency, generator mechanical efficiency, working fluid mass flow rate, enthalpies at the points 5 and 6, respectively.

The energy efficiency of the integrated system is expressed as:

$$\eta_{int,sys} = \frac{\dot{W}_{net}}{\dot{Q}_{ev}} \quad (21)$$

where  $\dot{Q}_{ev}$  is the input heat to the ORC and is given by:

$$\dot{Q}_{ev} = \dot{m}_8 (h_5 - h_8) \quad (22)$$

where  $\dot{m}_8$ ,  $h_5$  and  $h_8$  are the working fluid mass flow rate, enthalpies at the points 5 and 8, respectively.

The exergy efficiency of the integrated system is expressed as:

$$\psi = \frac{\dot{W}_{net}}{\dot{E}x_{in-eva} + \dot{E}x_{in-con} + \dot{E}x_{solar}} \quad (23)$$

where

$$\dot{E}x_{in-eva} = \dot{m}_3 [(h_3 - h_0) - T_0 (s_3 - s_0)] \quad (24)$$

$$\dot{E}x_{in-con} = \dot{m}_9 [(h_9 - h_0) - T_0 (s_9 - s_0)] \quad (25)$$

$$\dot{E}x_{solar} = \dot{I}\Psi = \dot{I} \left[ 1 - \frac{4}{3} \left( \frac{T_0 + 273}{T_{solar}} \right) + \frac{1}{3} \left( \frac{T_0 + 273}{T_{solar}} \right)^4 \right] \quad (26)$$

where  $\dot{E}x_{solar}$  is the exergy of solar radiation coming on the surface of the solar systems,  $\Psi$  is the exergy of solar radiation [19]. The reference environment state is taken to be  $T_0 = 30^\circ C$ ,

**Table 1 – Thermodynamics parameters of the integrated system.**

No	Fluid	Temperature (°C)	Pressure (kPa)	Mass flow rate (kg/s)	Enthalpy (kJ/kg)	Entropy (kJ/kg °C)	Specific ex. (kJ/kg)	Exergy (kW)
Ref.	H <sub>2</sub> O	30	101.3	–	125.8	0.44	–	–
1	H <sub>2</sub> O	40	200	0.5	167.7	0.57	0.79	0.4
2	H <sub>2</sub> O	60	200	0.5	251.3	0.83	5.98	2.99
3	H <sub>2</sub> O	91.61	200	0.5	383.8	1.21	23.36	11.68
5	Ammonia	80	2000	0.08	1625	5.45	19.31	1.55
6	Ammonia	45	1750	0.08	1493	5.12	50.75	4.06
7	Ammonia	30	1750	0.08	342	1.49	101.7	8.14
8	Ammonia	31	2000	0.08	346.9	1.5	101.2	8.1

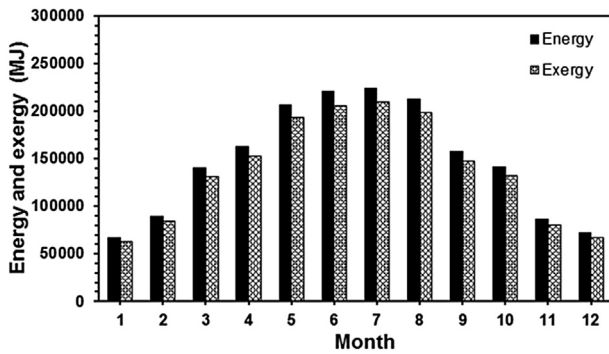


Fig. 5 – Total energy and exergy distributions of the solar radiation in Adana for the pond.

$P_0 = 101.3$  kPa and the surface temperature of the sun  $T_{\text{solar}} = 6000$  K.

## Results and discussion

Temperature, pressure, mass flow rate, enthalpy, entropy, specific exergy and exergy are given in Table 1. These values are used for the calculations to make the thermodynamic analysis.

The temperature of the storage zone of the pond that has a surface area  $300 \text{ m}^2$  is assumed to be  $64^\circ\text{C}$ . The inlet and outlet water temperatures to the exchanger-1 are assumed to be  $40^\circ\text{C}$  and  $60^\circ\text{C}$ , respectively. The temperature of the outlet water from the exchanger-1 is upgraded to  $91.61^\circ\text{C}$  by using the flat-plate collector that has a surface area  $250 \text{ m}^2$ .

The amount of incident solar radiation must be known in order to determine the performance of the integrated system. Therefore the average of the solar radiation data from the Meteorology Regional Directorate of Adana to 2010 and 2013 are used to reduce the margin of error in the calculations. Accordingly, the energy and exergy distributions of the solar radiation in Adana for the pond and collector are shown in Figs. 5 and 6, respectively.

As shown in Fig. 5, the maximum values of total solar energy and exergy for the pond are  $224430 \text{ MJ}$  and  $209387 \text{ MJ}$  in July while the minimum values are  $66807 \text{ MJ}$  and  $62608 \text{ MJ}$  in January, respectively.

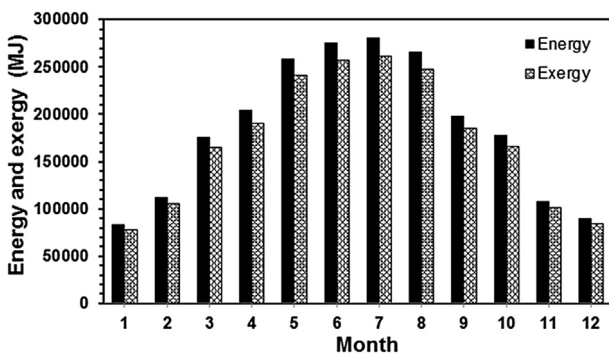


Fig. 6 – Total energy and exergy distributions of the solar radiation in Adana for the collectors.

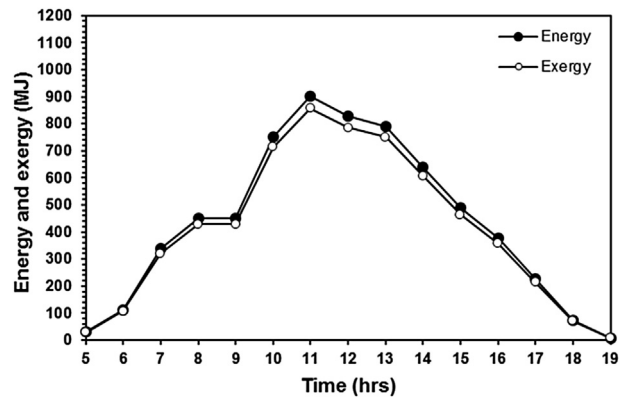


Fig. 7 – Energy and exergy distribution of the solar radiation in Adana for the pond at 15th July.

As shown in Fig. 6, the maximum values of total solar energy and exergy for the collector are  $280537 \text{ MJ}$  and  $261734 \text{ MJ}$  in July respectively while the minimum values are  $83508 \text{ MJ}$  and  $78260 \text{ MJ}$  in January respectively.

As seen in Figs. 5 and 6, the amount of the incident solar energy and its exergy of the collectors is greater than that incident on the solar pond due to the tilt angle of the collectors.

Figs. 7 and 8 shows that the solar radiation is reached at 5 o'clock in the morning until 19 in the evening and get the maximum energy and exergy values at 11 o'clock at 15th July.

Accordingly, the highest value of solar energy for the pond and the collectors were  $902 \text{ MJ}$  and  $1128 \text{ MJ}$  while the highest value of solar exergy  $857 \text{ MJ}$  and  $1072 \text{ MJ}$  respectively at 15th July. As seen here in the figures, the exergy of the solar radiation is less than the corresponding energy due to the fact that energy is conserved but not exergy according to the second law of the thermodynamic. So, some exergy is destructed due to exergy losses of the solar radiation coming from Sun to the Earth. As seen in Figs. 5 and 6, the lowest exergy contents appear in January and the highest ones in July. Of course, the surroundings temperature plays a key role in a year. And also, Figs. 7 and 8 show the exergy of the daily solar radiation reaching on the surface of the solar pond and collectors are less than the corresponding energy due to the fact that second

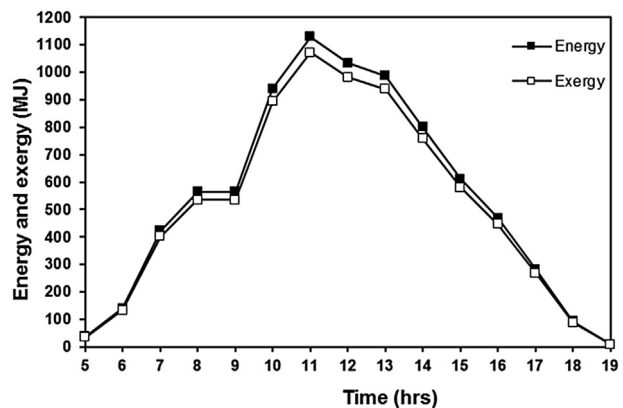


Fig. 8 – Energy and exergy distribution of the solar radiation in Adana for the collector at 15th July.

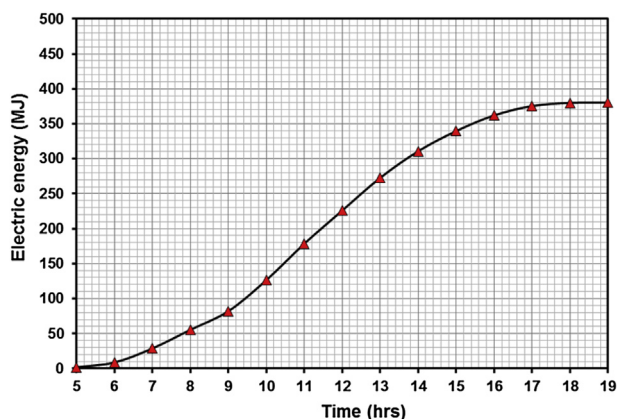


Fig. 9 – Accumulation of the generated electric energy for 15th July.

law of the thermodynamics. It is important to mention that the shape of the energy and exergy distributions follow the solar irradiation profiles closely.

Thermal energy is converted into electrical energy by using the Organic Rankine cycle which is working with an organic fluid with a liquid–vapor phase change at a lower temperature than the water–steam phase change. Thus the low-temperature heat is converted into useful work. The organic fluids allow Rankine cycle heat recovery from lower temperature sources such as solar pond and collectors. In the real cycle, only a part of the energy recoverable from the pressure difference is transformed into useful work during the expansion in the turbine. The remaining part is converted into heat and is lost. Therefore, the presence of irreversibility lowers the cycle efficiency and mainly effect on the amount of the electric generation.

When the efficiencies of the turbine and generator are considered as to be 90%, it is calculated that 380 MJ electrical energy can be generated by the system for a day as shown in Fig. 9.

As shown in Fig. 10, total mass of produced hydrogen by the system is 2.25 kg. It is obvious that the most of the hydrogen production took place at noon hours because of the strong effect of the incident radiation. As expected, in the

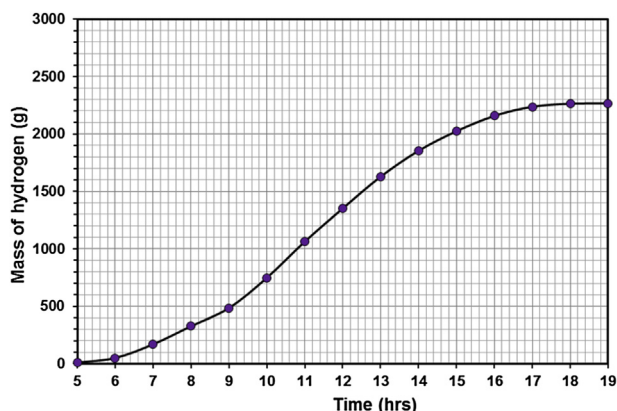


Fig. 10 – Accumulation of the produced hydrogen for 15th July.

morning and afternoon low hydrogen production took place due to the weak solar radiation.

## Conclusions

In this study, hydrogen production performance of an integrated thermal system that consists of a solar pond, flat-plane solar collectors and an ORC was examined. Consequently, solar pond has increased the temperature of the inlet water to the plane solar collectors in order to increase the thermal performance of the system. It was observed that a significant amount of electrical power can be generated in the ORC system by increasing the temperature of the water within a short time. The generated power in the model system was used for hydrogen production by electrolysis system. A significant proportion of hydrogen was produced as a final output of the system. One of the most important advantages of such an integrated system, the excess thermal energy in the summer months can be used to produce hydrogen production for future use. Consequently, more electricity and more hydrogen is produced if the heat losses and destruction of the system can decrease. Finally, the produced hydrogen, renewable and clean energy carrier, can be used as fuel in homes and vehicles.

## REFERENCES

- [1] Dincer I, Rosen MA. Thermal energy storage: systems and applications. 2nd ed. New York: John Wiley and Sons; 2011.
- [2] Karakilcik M, Dincer I, Rosen M. Performance investigation of a solar pond. *Appl Therm Eng* 2006;26:727–35.
- [3] Bozkurt I, Karakilcik M. The daily performance of a solar pond integrated with solar collectors. *Sol Energy* 2012;86:1611–20.
- [4] Abh Date, Yaakob Y, Ash Date, Krshnapillai S, Akbarzadeh A. Heat extraction from non-convective and lower convective zones of the solar pond: a transient study. *Sol Energy* 2013;97:517–28.
- [5] Saleh AM. Modeling of flat-plate solar collector operation in transient states. Master Thesis in Science Engineering. Indiana: Purdue University Fort Wayne; 2012.
- [6] Farahat S, Sarhaddi F, Ajam H. Exergetic optimization of flat-plate solar collectors. *Renew Energy* 2009;34:1169–74.
- [7] Dikici A, Akbulut A. Performance characteristics and energy-exergy analysis of solar-assisted heat pump system. *Build Environ* 2008;43:1961–72.
- [8] Ahmadi P, Dincer I, Rosen MA. Multi-objective optimization of an ocean thermal energy conversion system for hydrogen production. *Int J Hydrogen Energy* 2015;4:7601–8.
- [9] Bicer Y, Dincer I. Development of a new solar and geothermal based combined system for hydrogen production. *Sol Energy* 2016;127:269–84.
- [10] Bozoglan E, Midilli A, Hepbasli A. Sustainable assessment of solar hydrogen production techniques. *Energy* 2012;46:85–93.
- [11] Joshi AS, Dincer I, Reddy BV. Effects of various parameters on energy and exergy efficiencies of a solar thermal hydrogen production system. *Int J Hydrogen Energy* 2016;41:7997–8007.
- [12] Yaakob Y, Leblanc J, Date A, Akbarzadeh A. Heat extraction from salinity-gradient solar ponds using external heat

- exchangers. In: Solar 2010, the 48th AuSES Annual Conference, 1–3 December 2010, Canberra, ACT, Australia; 2010.
- [13] Ding LC, Akbarzadeh A, Date A. Transient model to predict the performance of thermoelectric generators coupled with solar pond. *Energy* 2016;103:271–89.
- [14] Cengel YA. Heat and mass transfer. 3rd ed. Mc Graw Hill; 2006. p. 680–1.
- [15] Ioardanou G. Flat-plate solar collectors for water heating with improved heat transfer for application in climatic conditions of the Mediterranean Region. Durham University; 2009. PhD Thesis.
- [16] Duffie JA, Beckman WA. Solar engineering of thermal process. 2nd ed. New York: Wiley Interscience; 1991.
- [17] Mago PJ, Chamra LM, Somayaji C. Performance analysis of different working fluids for use in organic Rankine cycle. *J Power Energy Proc IMechE* 2006;221:255–63.
- [18] Tchanche BF, Gr Lambrinos, Frangoudakis A, Papadakis G. Exergy analysis of micro-organic Rankine power cycles for a small scale solar driven reverse osmosis desalination system. *Appl Energy* 2010;87:1295–306.
- [19] Petala R. Exergy of undiluted thermal radiations. *Sol Energy* 2003;74:469–88.